

Chapter 6

Mechanical Properties of 3-D LENS and PBF Printed Stainless Steel 316L Prototypes

Wei-Yang Lu, Nancy Yang, Joshua Yee, and Kevin Connelly

Abstract Laser Engineered Net Shaping (LENS) and Powder Bed Fusion (PBF) are 3-D additive manufacturing (AM) processes. They are capable of printing metal parts with complex geometries and dimensions effectively. Studies have shown that AM processes create metals with distinctive microstructure features and material properties, which are highly dependent on the processing parameters. The mechanical properties of an AM material may appear to be similar to the corresponding wrought material in some way. This investigation focuses on the relationships among AM process, microstructure features, and material properties. The study involves several AM SS316L components made from 3D LENS and PBF printing. Specimens were taken from different locations and orientations of AM components to obtain the associated tensile properties, including yield, strength, and ductility, and to conduct microstructure analyses.

Keywords Additive manufacture • LENS • PBF • SS316L

6.1 Introduction

In a recent study of AM SS316L properties of a 3-D LENS deposited hexagon [1], tensile testing was performed for specimens oriented along the build direction (BD) and the transverse direction (TD). The results show that yield stress (YS) and ultimate tensile strength (UTS) of 3D LENS deposits are generally higher than nominal values for the wrought SS316L. As for ductility, LENS TD specimens were about the same as wrought SS316L; however, the elongation of BD specimens was notably low and varied greatly. Microstructure analyses suggest that the phenomena are caused by the inter-pass structure of the material. The BD specimen that had low strain to failure value was failed by inter-pass delamination, where lack-of-fusion defects are observed on the fracture surface of the specimen.

This work extends the investigation to SS316L prototypes of a different AM process PBF plus another LENS hexagon deposited from a new set of process parameters.

6.2 AM SS316L Prototypes

Figure 6.1a displays a substrate of prototypes 3D printed from a PBF machine ProX300 at Sandia National Laboratories/CA. Among these prototypes, a cylinder and a 3-tier hexagon, marked as 1 and 2 on the figure, were used for this study. The coordinate of each prototype was defined as the same as the machine reference frame: x-axis is the roller direction, y-axis is the transverse direction, and z-axis is the build direction. The diameter of the cylinder was 1.0 inch, and the height was 2.0 inch. For the hexagon, its cross-section (y-z plan) is shown in Fig. 6.1b. The dimensions were the same as the LENS hexagon, described in [1], where the distance between the outside edges of two opposite sides was 2.0 inch and the height was also 2.0 inch. Printing parameters and conditions are listed in Table 6.1.

A LENS fabricated short hexagon is shown in Fig. 6.1c. The dimensions were the same as the PBF hexagon described above but only had two tiers, where the total height was 1.2 inch instead of 2.0 inch. It was 3D printed from a LENS machine Optomec750 at UC Irvin. The hatch pattern was the same as that in [1], where the hatch lines of two adjacent layers were at 90°. They were parallel to either x or y axis. A new set of processing parameters is shown in Table 6.2.

W.-Y. Lu (✉) • N. Yang • J. Yee • K. Connelly
Sandia National Laboratories, Livermore, CA 94551-0969, USA
e-mail: wlu@sandia.gov

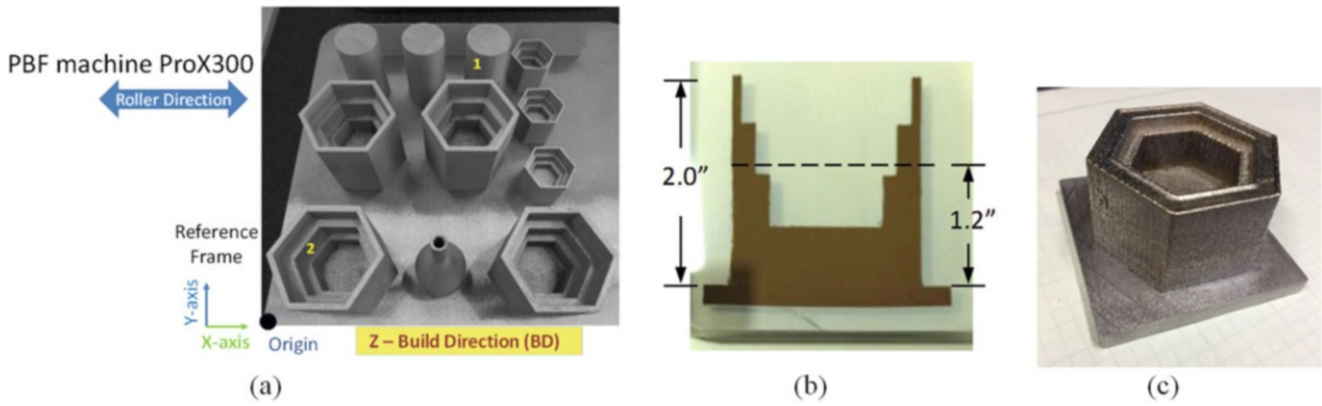


Fig. 6.1 AM SS316L prototypes. (a) 3D printed prototypes; (b) Hexagon cross-section in the y-z plan; (c) LENS short hexagon

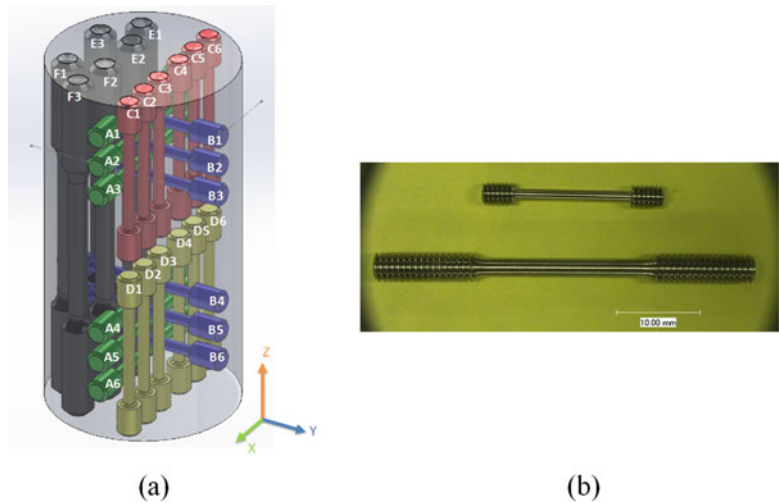
Table 6.1 PBF processing parameters

Laser power	Power layer thickness	Laser scan speed
41% (of 500 W)	40 mm	1200 mm/s

Table 6.2 LENS short hexagon processing parameters

Laser power	Speed
400 W	16.3 mm/s

Fig. 6.2 Specimens machined from cylinders. (a) ID, location and orientation of each specimen; (b) Two specimen sizes



6.3 Tensile Specimens

Tensile specimens were extracted from prototypes. Figure 6.2a shows the location, orientation, and size of each specimen machined from the PBF cylinder. These specimens could be gathered into five groups: Group A was specimens aligned in x-direction; Group B was in y-direction; Groups C, D and E were in z-direction. Again, x-, y-, and z-axes are referred to the machine reference frame. Two sizes of specimens were included, shown in Fig. 6.2b. The large size specimens, Group E, had a gage diameter of 0.1 inch with a total length of 2.0 inch. All others, Groups A – D, were the small size, which had the dimensions of 0.06 inch and 1.0 inch for gage diameter and total length, respectively. Furthermore, Group C and half of Groups A and B (A1 – A3 and B1 – B3) were from the top half of the cylinder, while Group D and other half of Groups A and B (A4 – A6 and B4 – B6) were from the bottom half of the cylinder.

Specimens in x-, y-, and z-directions were also machined from the hexagons. Due to the geometry, the specimens oriented in the build direction (z) were close to the wall; the transverse specimens, oriented in the x- and y-directions, were close to the base. Additional transverse off-axis specimens were also obtained. Their orientation x' and y' were 30° clockwise relative to x and y.

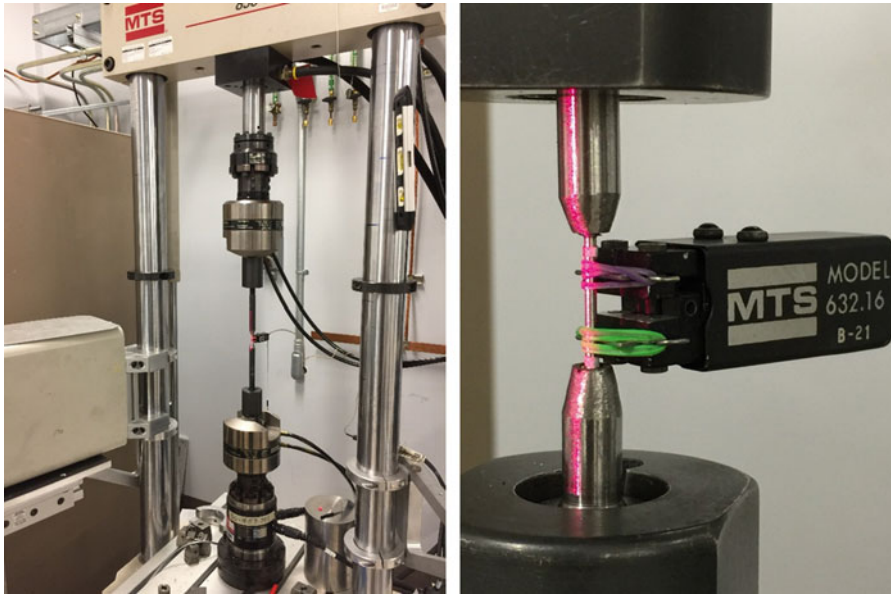


Fig. 6.3 Laser and mechanical extensometers are used to measure large and small deformations, respectively

6.4 Experimental Setup

Tensile tests were conducted on a MTS Bionix System, as shown in Fig. 6.3. The loading was quasi-static, at a strain rate of about $0.5 \times 10^{-3} \text{ s}^{-1}$. The specimen was self-aligned with ball-and-socket joints in the loading train. Both laser and mechanical extensometers were used to measure the deformation at the gage section. The mechanical extensometer measures deformation up to 20% from a gage length of 0.3 inch. Since it could not cover the whole deformation of SS316L specimens, the high resolution mechanical extensometer was used for small strain measurement only a laser extensometer was needed to capture the total deformation with a lower resolution. Thin reflection tapes were mounted on the gage section as targets for the laser extensometer, which were separated at least 0.45 inch.

6.5 Experimental Results

6.5.1 PBF Cylinder

The engineering stress-strain curves are plotted in Fig. 6.4a. There are 14 curves, about three specimens per each group except Group E with only two. The curves are clearly clustered in three bundles, which correspond to specimens in three orientations. All specimens along the build direction z, including Groups C, D and E, have a lower yield stress (YS) and ultimate strength (UTS); also they are relatively flat, indicating limited work hardening. Those specimens in the transverse directions, Groups A and B, have a similar UTS, but Group A, x-direction, shows a larger elongation while Group B, y-direction, has a higher hardening rate. The anisotropic behavior of the material is obvious.

In order to examine the data of z-direction specimens more closely, the hardening portion of the curves in Fig. 6.4a was magnified and shown in Fig. 6.4b. Two noticeable trends are displayed. One, the stress-strain curves of Group D specimens are all lower than Group C curves. Since Groups C and D correspond to top and bottom half of the cylinder, the result suggests that material properties may vary slightly along the build direction. The other is that Groups C and E curves are

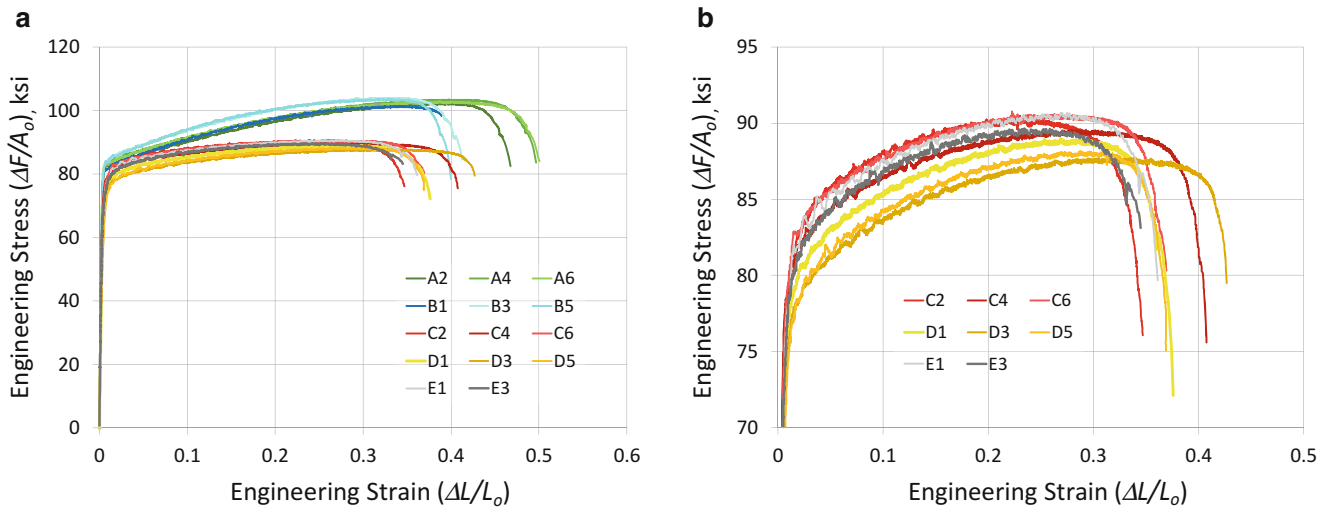


Fig. 6.4 Engineering stress-strain curves of specimens from the PBF cylinder. (a) A, B and C-D-E correspond to on-axis X, Y and Z curves; (b) Magnified hardening portion of Z curves

Table 6.3 Tensile parameters of PBF cylinder and wrought SS316L

Specimen	YS (ksi)	UTS (ksi)	Elongation (%)
A2	79	102	47
A4	80	103	50
A6	82	103	50
B1	80	101	39
B3	82	104	41
B5	81	104	40
C2	58	90	35
C4	74	90	41
C6	69	89	37
D1	63	89	38
D3	62	88	43
D5	55	88	37
E1	67	91	36
E3	68	90	35
Wrought [2]	25	70	40

generally overlap, which shows large and small size specimens have the same result. The small size specimen is adequate for AM material characterization.

The numerical values of these material parameters are listed on Table 6.3. Typical wrought SS316L properties are also included in the Table [2]. In comparison, YS and UTS of PBF printed SS316L are much higher than the wrought material. Although elongations are comparable, it is about 10–15% lower in the PBF build direction. Within a specimen group, the YS and UTS are quite consistent. The elongation, however, appears to have a relatively large scatter, especially within Groups C and D. Take Group C for example, the elongation of specimen C4 is far greater than C2 and C6. The result seems to correlate with the location of each specimen, that is C4 is closer to the center of the cylinder and C2 and C6 are closer to the edge. The result of Group D supports such correlation. The phenomenon may be due to localized thermal transport and heat distribution [1], which vary between center and edge.

Obviously, more experimental data are needed to statistically confirm the location effects on AM materials that are suggested by the limited data presented in current experiments of PBF cylinder.

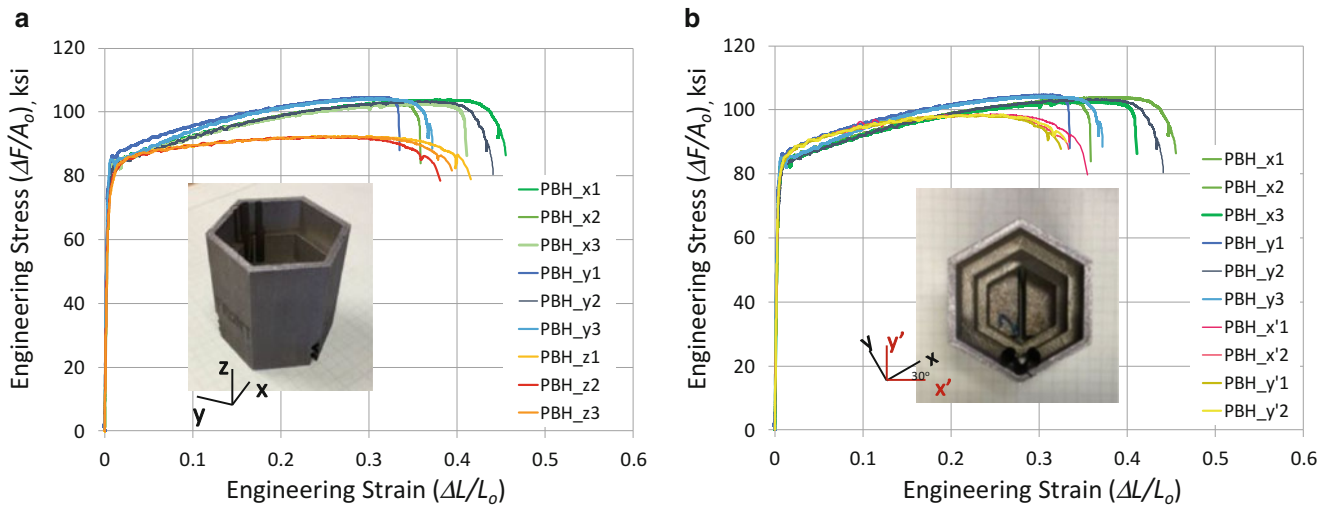


Fig. 6.5 Engineering stress-strain curves of specimens from the PBF hexagon. (a) X, Y and Z on-axis curves; (b) On-axis and off-axis X and Y curves

6.5.2 PBF Hexagon

The engineering stress-strain curves of on-axis specimens are plotted in Fig. 6.5a. Specimens in each orientation displayed distinctive hardening and elongation. These curves are consistent with those of PBF cylinder. Specimens of the same orientation show the same curve shape and material parameter values. There is one outlier, specimen PBH_y2, which is in the y-direction group but appears to follow the hardening behavior of those in the x-direction.

Figure 6.5b displays the engineering stress-strain curves of all transverse specimens of the PBF hexagon. The curves of two off-axis groups, x' and y' , gather together exhibiting no difference. They are clearly distinctive from on-axis groups x and y , showing lower UTS and necking at a relatively low strain.

6.5.3 LENS Short Hexagon

The engineering stress-strain curves are shown in Fig. 6.6a and the material parameters are listed in Table 6.4. As shown in the figure, there are only two clusters for three groups of on-axis specimens. The engineering stress-strain curves of x and y group overlap displaying no difference between these two groups. It suggests that the material is transversely isotropic, but needs additional transverse off-axis data to confirm.

Comparing to the previous study [1], shown in Fig. 6.6b and Table 6.5, the current material is much improved, especially the properties in the build direction. The stress-strain curves are consistent and there is no premature failure, which indicates fabrication defects are controlled with the new set of processing parameters.

6.6 Fractography

The failure surfaces of PBF cylinder specimens were examined. Figure 6.7 shows a typical specimen from each group. At the low magnification $100\times$, voids are visible. The size and number of void do not appear to correlate with the strain to failure. As shown in Fig. 6.7d, specimen D3 displays a lot more large-size voids than C4 but the elongation is slightly longer. At the higher magnification $2000\times$, all failure surfaces exhibit typical ductile failure, featuring a small cell size dimpled fracture surface [1].

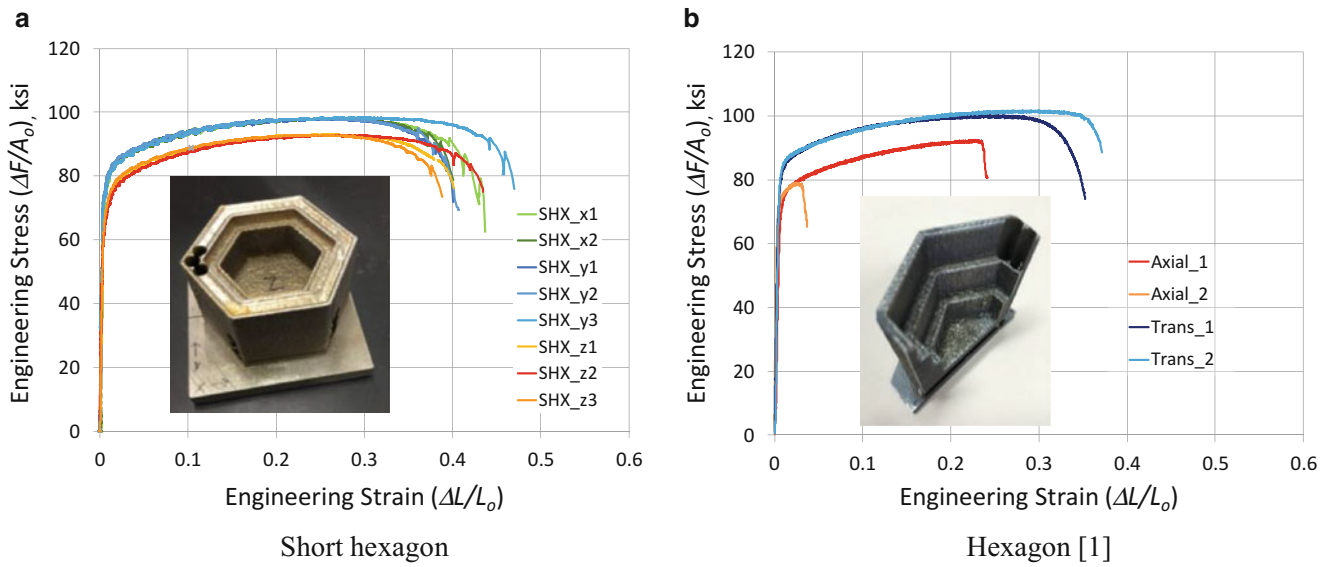


Fig. 6.6 Engineering stress-strain curves of specimens from the LENS short hexagon. (a) Short hexagon; (b) Hexagon [1]

Table 6.4 Tensile parameters of LENS short hexagon

Specimen	YS (ksi)	UTS (ksi)	Elongation (%)
SHX_x1	70	98	44
SHX_x2	71	98	39
SHX_y1	72	98	40
SHX_y2	73	98	41
SHX_y3	71	98	48
SHX_z1	61	93	40
SHX_z2	60	93	43
SHX_z3	61	93	39

Table 6.5 Tensile parameters of LENS hexagon [1]

Specimen	YS (ksi)	UTS (ksi)	Elongation (%)
Axial_1	65	92	26
Axial_2	70	79	4
Trans_1	70	100	35
Trans_2	69	102	38

6.7 Summary and Conclusion

Tensile testing was conducted for specimens taken from PBF and LENS prototypes. Depending on the process, AM SS316L shows various anisotropic behaviors.

The PBF cylinder and hexagon included in this study were from the same substrate but relatively far apart. Even with different geometries, their bulk tensile properties are generally consistent.

Two different specimen sizes were considered. Their results are also consistent, which indicates using the small size specimen is adequate.

Within a PBF prototype, there are minor variations of mechanical properties with respect to location. This collaborates the suggestion that it is “a result of the localized thermal transport and heat distribution” [1].

3-D LENS and PBF prints exhibit cellular solidified cells with extremely fine arm spacing. Fractography of PBF cylinder sample shows the ductile dimple failure.

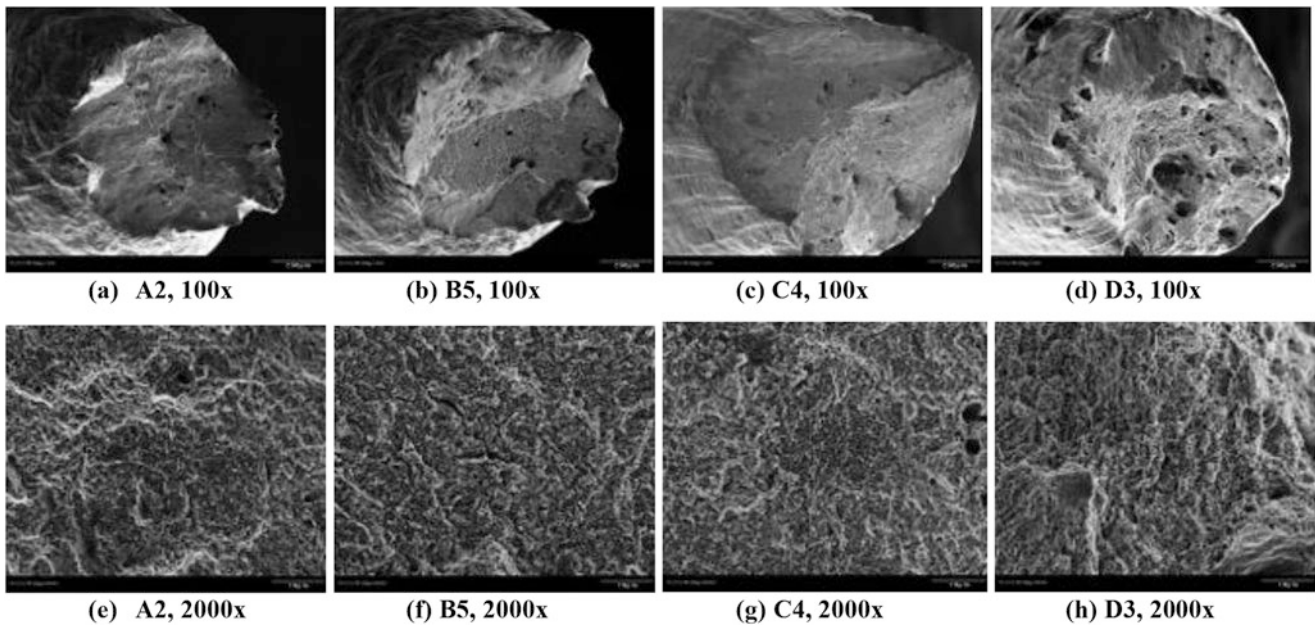


Fig. 6.7 SEM micrograph of failure surfaces. (a) A2, 100 \times ; (b) B5, 100 \times ; (c) C4, 100 \times ; (d) D3, 100 \times ; (e) A2, 2000 \times ; (f) B5, 2000 \times ; (g) C4, 2000 \times ; (h) D3, 2000 \times

Microstructural analyses of failed specimens of PBF hexagon and LENS short hexagon are current underway. Also, tensile testing of LENS cylinder and 3-tier hexagon is being performed to compare with PBF data.

Acknowledgements The authors would like to acknowledge the LENS hexagon provided by University of California, Irvine. Sandia National Laboratories is a multi-mission laboratory managed and operated by Sandia Corporation, a wholly owned subsidiary of Lockheed Martin Corporation, for the U.S. Department of Energy's National Nuclear Security Administration under contract DE-AC04-94AL85000.

References

1. Yang, N., et al.: Process-structure-property relationships for 316L stainless steel fabricated by additive manufacturing and its implication for component engineering. *J. Therm. Spray Technol.* (2016). doi:[10.1007/s11666-016-0480-y](https://doi.org/10.1007/s11666-016-0480-y)
2. www.AZOM.com